Eur. Phys. J. A **23**, 11–17 (2005)
DOI 10.1140/epja/i2004-10074-0

THE EUROPEAN PHYSICAL JOURNAL A

Halo or skin in the excited states of some light mirror nuclei

J.G. Chen[1,2,3,a], X.Z. Cai[1], W.Q. Shen[1], Y.G. Ma[1], Z.Z. Ren[4], H.Y. Zhang[1], W.Z. Jiang[1], C. Zhong[1], Y.B. Wei[1,3], W. Guo[1,3], X.F. Zhou[1,3,5], K. Wang[1,3], and G.L. Ma[1,3]

[1] Shanghai Institute of Applied Physics, Chinese Academy of Sciences, Shanghai 201800, PRC
[2] College of Sciences, Zhejiang Forestry University, Hangzhou 311300, PRC
[3] Graduate School of the Chinese Academy of Sciences, PRC
[4] Department of Physics, Nanjing University, Nanjing 210008, PRC
[5] College of Sciences, Ningbo University, Ningbo 315211, PRC

Received: 6 June 2004 / Revised version: 2 September 2004 /
Published online: 1 December 2004 –
Communicated by C. Signorini

Abstract. The properties of three pairs of mirror nuclei ^{13}N-^{13}C, ^{15}N-^{15}O and ^{21}Na-^{21}Ne (these mirror nuclei are all made of a good inert core plus an unpaired valence nucleon) are investigated by using the nonlinear relativistic mean-field (RMF) theory. It is found that the calculated binding energies with two different parameter sets are very close to the experimental ones for both the ground states and the excited states except for the large deformed nuclei. The calculations show that the $2s_{1/2}$ excited states of ^{15}N and of ^{21}Na are both weakly bound with a proton halo and a proton skin (or a pigmy proton skin), respectively. In addition, the $1d_{5/2}$ excited state of ^{13}C and the $2s_{1/2}$ excited state of ^{15}O are also weakly bound with a neutron skin, respectively. The ratio of the valence nucleon radius to matter radius is deduced and it can be regarded as an additional criterion for the existence of exotic structure. The unbound $2s_{1/2}$ and $1d_{5/2}$ excited states of ^{13}N are also discussed.

PACS. 21.10.Gv Mass and neutron distributions – 21.60.Jz Hartree-Fock and random-phase approximations – 21.10.Dr Binding energies and masses – 27.20.+n $6 \leq A \leq 19$

1 Introduction

The nuclei far from the β-stability line have been studied widely and exotic structures (halos or skins) in the ground states were found in many of them [1–26]. However, studies on the halo in the excited states of nuclei near the β-stability line are relatively scarce. Morlock *et al.* were the first to shed light on the existence of proton halo in the excited state of stable nuclei [27]. They observed that in a proton capture reaction at low energies, *i.e.*, ^{16}O (p, γ) ^{17}F, the low-energy S-factor is dominated by a transition to the first excited state ($2s_{1/2}$) in ^{17}F. They found that the S-factor increases strongly with decreasing incident energies and this indicates the existence of a proton halo in the $2s_{1/2}$ excited state of ^{17}F. Ren *et al.* investigated ^{17}F using the nonlinear relativistic mean-field (RMF) theory and arrived the same conclusion [28]. Liu *et al.* and Lin *et al.* showed the existence of a neutron halo in the excited states of nuclei ^{12}B and ^{13}C [29,30]. They extracted the root-mean-square (RMS) radii of the last neutron in different states of nuclei by a transfer reaction and indicated that the second and the third excited states in ^{12}B and the first excited state in ^{13}C are neutron halo states, whereas the third excited state in ^{13}C is a neutron skin state. Ren *et al.* calculated the nucleon density distributions for the excited states of ^{13}C, ^{12}B, ^{16}N and ^{17}O with RMF and gave the theoretical proof for the halo [31]. Moreover, K. Arai *et al.* investigated the more complicated halos in the second excited state of ^{6}Li with a fully microscopic three-cluster model and predicted that ^{6}Li has a conspicuous halo-like structure formed by a neutron and a proton surrounding the α core, *i.e.*, deuterium halos [32]. Li *et al.* measured the angular distributions of the exchange reaction ^{1}H (^{6}He, ^{6}Li) n in the reverse kinematics with a secondary ^{6}He beam at the energy of 4.17 MeV/u and provided experimental evidence of deuterium halos in the second excited state of ^{6}Li [33]. Study of halo or skin structures in the excited states is of great interest and it does not require a big facility for the production of radioactive beams.

Since the RMF theory has been applied with considerable success to the quantitative description of nuclear properties in the ground states and to the prediction for the halo in the excited states [2,5,11,28,31,34–40], it is also interesting to give a theoretical prediction for halo or skin in the excited states of other nuclei with the RMF

[a] e-mail: Chenjg@sinr.ac.cn

model. In this paper, we investigate whether there exists a halo or a skin in some excited states of ^{13}N-^{13}C, ^{15}N-^{15}O and ^{21}Na-^{21}Ne by using the frame of the nonlinear RMF model.

This paper is organized as follows. In sect. 2, we give a brief description of the RMF theory. The calculations and the results are presented in sect. 3. In sect. 4 we give a discussion of the results. Section 5 contains the conclusion.

2 The RMF theory

We make a very brief description of the RMF theory (details can be found in refs. [2,5,11,34,34–40]). We start from the local Lagrangian density for interacting nucleons, σ-, ω-, and ρ-mesons and photons, which are used to obtain the RMF equations:

$$\begin{aligned}\pounds = {} & \bar{\Psi}(i\gamma^\mu\partial_\mu - M)\Psi - g_\sigma\bar{\Psi}\sigma\Psi - g_\omega\bar{\Psi}\gamma^\mu\omega_\mu\Psi \\ & - g_\rho\bar{\Psi}\gamma^\mu\rho_\mu^a\gamma^a\Psi + \frac{1}{2}\partial^\mu\sigma\partial_\mu\sigma - \frac{1}{2}m_\sigma^2\sigma^2 \\ & - \frac{1}{3}g_2\sigma^3 - \frac{1}{4}g_3\sigma^4 - \frac{1}{4}\Omega^{\mu\nu}\Omega_{\mu\nu} + \frac{1}{2}m_\omega^2\omega^\mu\omega_\mu \\ & - \frac{1}{4}R^{a\mu\nu}R_{\mu\nu}^a + \frac{1}{2}m_\rho^2\rho^{a\mu}\rho_\mu^a - \frac{1}{4}F^{\mu\nu}F_{\mu\nu} \\ & - e\bar{\Psi}\gamma^\mu A^\mu\frac{1}{2}\big(1-\tau^3\big)\Psi,\end{aligned}$$

with

$$\begin{aligned}\Omega^{\mu\nu} &= \partial^\mu\omega^\nu - \partial^\nu\omega^\mu, \\ R^{a\mu\nu} &= \partial^\mu\rho^{a\nu} - \partial^\nu\rho^{a\mu}, \\ F^{\mu\nu} &= \partial^\mu A^\nu - \partial^\nu A^\mu,\end{aligned}$$

where σ, ω_μ and ρ_μ^a denote the meson fields and their masses are given by m_σ, m_ω and m_ρ, respectively. The nucleon fields and rest masses are denoted by Ψ and M, respectively. A is the photon field which is responsible for the electromagnetic interaction. The effective coupling constants between mesons and nucleons are g_σ, g_ω, and g_ρ, respectively. The coupling constants of the nonlinear σ terms are called g_2 and g_3. τ^a represents the isospin Pauli matrices and τ^3 is the third component of τ^a. Under the mean-field approximation, the meson fields are considered as classical fields and they are replaced by their expectation values in vacuum. Using procedures similar to those of refs. [2,5,35,37], we obtain a set of coupled equations for mesons, nucleons, and photons. They are solved consistently in coordinate space by iteration. There are many well-tested nonlinear RMF parameter sets, two sets of which, NL3 [41] and NLZ [7], are chosen for numerical calculations in this work. They are two typical forces in the RMF model and it is expected that other forces will lead to very similar results. For both parameter sets, we use the term $0.75 \times 41A^{1/3}$ to evaluate the correction of the additional energy due to the motion of the center of mass [9].

3 Calculations and results

The experimental study performed by Liu *et al.* indicated that a neutron halo and a neutron skin can form in the $2s_{1/2}$ and in the $1d_{5/2}$ excited states of ^{13}C, respectively [29]. Theoretical study on the $2s_{1/2}$ of ^{13}C has been done too [31]; but there is no relevant theoretical RMF study either on the $1d_{5/2}$ excited state of ^{13}C or on the excited states of ^{13}N, of ^{15}N-^{15}O and of ^{21}Na-^{21}Ne, so we give the corresponding theoretical prediction for them here.

The three pairs of mirror nuclei ^{13}N-^{13}C, ^{15}N-^{15}O and ^{21}Na-^{21}Ne have two similar characters. Firstly, all of them are stable and proton or neutron excess is relatively small, thus a halo or a skin can hardly exist in their ground states; secondly, these nuclei are composed of a good inert core plus an unpaired valence nucleon, which is relatively easily excited. Both experiments and model calculations show that the two excited states, $2s_{1/2}$ and $1d_{5/2}$ in the odd-A nuclei of $A = 13, 15$ are predominant single-particle levels relative to the core states [42]. Hence, we restrict our attention only to the $2s_{1/2}$ and the $1d_{5/2}$ excited states of ^{13}N-^{13}C and ^{15}N-^{15}O in the present article and the other excited states will not be considered. For the heavier mirror nuclei ^{21}Na-^{21}Ne, just the $2s_{1/2}$ excited state is calculated.

The three couples of mirror nuclei are calculated in the frame of the spherical RMF code. The core nuclei ^{12}C (the common core nucleus of ^{13}N and ^{13}C), ^{14}C (the core nucleus of ^{15}N) and ^{14}O (the core nucleus of ^{15}O) were calculated using the deformed RMF model and it was found that their deformations are very small. The heavier inert core (^{20}Ne) of ^{21}Na-^{21}Ne may be largely deformed [9]. However it is believed that the spherical model can be used to describe the properties of deformed nuclei as an approximation. It is well known that ^{10}Be (the core nucleus of ^{11}Be) is largely deformed, however Tanihata *et al.* still calculated ^{11}Be by using the spherical-shell model and obtained a satisfactory approximation [43].

We select ^{15}N as an example to explain the details of the calculations. First, we calculate binding energy, single-particle levels, RMS radii of proton and neutron density distributions for the ground state of the core nucleus (^{14}C). Then we calculate the properties of the ground state of ^{15}N by assuming that the last proton occupies the $1p_{1/2}$ state. Finally the properties of the first or of the second excited states are obtained by assuming that the last proton occupies the $1d_{5/2}$ or $2s_{1/2}$ state. Every step is a self-consistent RMF calculation. The total binding energy, separation energy, single-particle energy, radii, and wave function of each nucleon are obtained and root-mean-square radius of the last neutron can be calculated by its wave function.

The calculated results for ^{15}N-^{15}O obtained with parameter sets NL3 and NLZ are summarized in tables 1 and 2, respectively. The results for ^{21}Na-^{21}Ne and ^{13}N-^{13}C with NL3 are listed in tables 3 and 4, respectively, and those with NLZ are omitted, since NLZ will give almost the same results as those of NL3. In all the tables, $nL_J(_{LP})$ denotes the quantum number of the state occupied by the last nucleon. $B_{\rm exp.}$ [44–46] and B represent experimental and theoretical binding energies, respectively. The root-mean-square (RMS) radii of matter, proton, neutron, and the last nucleon density distributions are denoted by

Table 1. The RMF results for ^{15}N-^{15}O obtained with NL3 The states with the symbols "GS", "$ES1$" and "$ES2$" denote the ground states, the first and the second excited states, respectively. The units of binding energies and of single-particle energies are in MeV and those of various RMS radii and of the corresponding differences between proton RMS radii and neutron ones are in fm. Other details can be found in text.

	^{15}N			^{15}O		
$nL_J(_{LP})$	$1p_{1/2}{}^{GS}$	$2s_{1/2}{}^{ES2}$	$1d_{5/2}{}^{ES1}$	$1p_{1/2}{}^{GS}$	$2s_{1/2}{}^{ES1}$	$1d_{5/2}{}^{ES2}$
$B_{\rm exp.}$	115.49	110.19	110.22	111.96	106.78	106.72
B	115.16	108.19	111.87	111.79	104.80	104.75
R_m	2.55	2.75	2.52	2.56	2.67	2.61
R_p	2.52	2.90	2.53	2.61	2.60	2.57
R_n	2.58	2.61	2.51	2.50	2.74	2.51
R_{LP}	2.87	4.79	3.47	2.83	4.30	3.38
$\varepsilon_{LP}(p/n)$	−11.22	−0.88	−1.25	−14.59	−3.58	−4.12
$\lvert R_p - R_n\rvert$	0.06	0.29	0.02	0.11	0.14	0.06
R_{LP}/R_m	1.13	1.74	1.38	1.11	1.61	1.30

Table 2. The RMF results for ^{15}N-^{15}O obtained with NLZ. Other details can be found in the caption of table 1 and in text.

	^{15}N			^{15}O		
$nL_J(_{LP})$	$1p_{1/2}{}^{GS}$	$2s_{1/2}{}^{ES2}$	$1d_{5/2}{}^{ES1}$	$1p_{1/2}{}^{GS}$	$2s_{1/2}{}^{ES1}$	$1d_{5/2}{}^{ES2}$
$B_{\rm exp.}$	115.49	110.19	110.22	111.96	106.78	106.72
B	116.00	110.24	111.28	112.53	105.34	104.09
R_m	2.60	2.82	2.58	2.61	2.78	2.59
R_p	2.57	2.95	2.59	2.67	2.73	2.62
R_n	2.63	2.71	2.58	2.55	2.86	2.56
R_{LP}	2.93	4.66	3.55	2.90	4.35	3.44
$\varepsilon_{LP}(p/n)$	−11.28	−1.67	−1.60	−8.75	−4.35	−4.60
$\lvert R_p - R_n\rvert$	0.06	0.24	0.01	0.12	0.13	0.06
R_{LP}/R_m	1.13	1.65	1.38	1.11	1.57	1.33

Table 3. The RMF results for ^{21}Na-^{21}Ne obtained with NL3. The states with the symbols "GS" and "$ES4$" denote the ground states and the fourth excited states, respectively. Other details can be found in the caption of table 1 and in text.

	^{21}Na		^{21}Ne	
$nL_J(_{LP})$	$1d_{5/2}{}^{GS}$	$2s_{1/2}{}^{ES4}$	$1d_{5/2}{}^{GS}$	$2s_{1/2}{}^{ES4}$
$B_{\rm exp.}$	163.08	160.65	167.41	164.62
B	158.00	152.75	162.39	156.50
R_m	2.76	2.86	2.75	2.84
R_p	2.81	2.98	2.72	2.77
R_n	2.69	2.73	2.77	2.90
R_{LP}	3.37	4.50	3.29	4.13
$\varepsilon_{LP}(p/n)$	−4.79	−1.09	−9.50	−5.15
$\lvert R_p - R_n\rvert$	0.12	0.25	0.05	0.13
R_{LP}/R_m	1.22	1.57	1.20	1.45

Table 4. The RMF results for ^{13}N-^{13}C obtained with NL3 (the results for the ground state and the first excited state ($2s_{1/2}$) of ^{13}C are taken from ref. [31]). The states with the symbols "GS", "$ES1$" and "$ES3$" denote the ground states, the first and the third excited states, respectively. Other details can be found in the caption of table 1 and in text.

	^{13}N			^{13}C		
$nL_J(_{LP})$	$1p_{1/2}{}^{GS}$	$2s_{1/2}{}^{ES1}$	$1d_{5/2}{}^{ES3}$	$1p_{1/2}{}^{GS}$	$2s_{1/2}{}^{ES1}$	$1d_{5/2}{}^{ES3}$
$B_{\rm exp.}$	94.11	91.74	90.56	97.11	94.02	93.26
B	94.12	92.86	91.46	98.09	92.48	92.49
R_m	2.38	/	/	2.40	2.48	2.41
R_p	2.46	/	/	2.33	2.21	2.24
R_n	2.29	/	/	2.45	2.71	2.53
R_{LP}	3.13	/	/	3.03	4.71	3.88
$\varepsilon_{LP}(p/n)$	−4.76	+0.52	+2.40	−8.44	−1.93	−0.33
$\lvert R_p - R_n\rvert$	0.17	/	/	0.12	0.50	0.29
R_{LP}/R_m	1.32	/	/	1.26	1.90	1.61

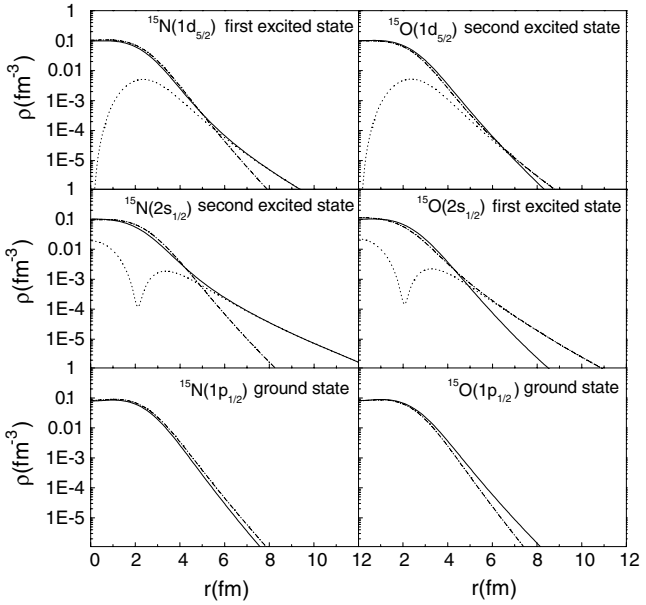

Fig. 1. The density distributions of proton, neutron, and the last nucleon for the ground state, the first and the second excited states in the mirror nuclei ^{15}N-^{15}O with NL3. Solid, dash-dotted, and dotted curves represent the density distributions of proton, neutron, and the last proton for ^{15}N or the last neutron for ^{15}O, respectively.

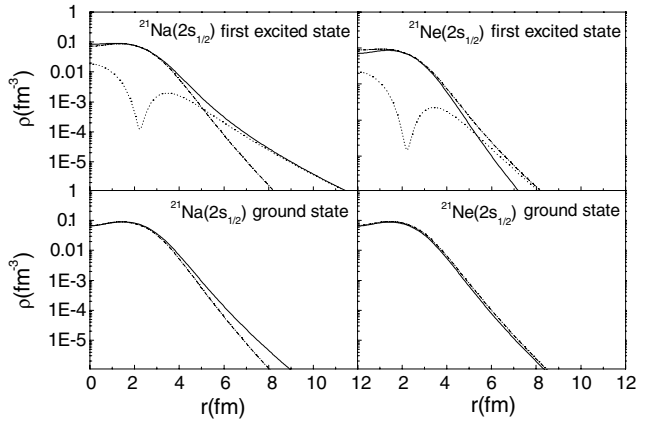

Fig. 2. The density distributions of proton, neutron, and the last nucleon for the ground state, the excited states in the mirror nuclei ^{21}Na-^{21}Ne with NL3. Solid, dash-dotted, and dotted curves represent the density distributions of proton, neutron, and the last proton for ^{21}Na or the last neutron for ^{21}Ne, respectively.

R_m, R_p, R_n, R_{LP}, respectively. $\varepsilon_{LP}(p/n)$ stands for the single-particle energy of the last nucleon. The difference of RMS radii between proton and neutron is represented by $|R_p - R_n|$. R_{LP}/R_m denotes the ratio of the valence nucleon RMS radius to the matter one. The density distributions of proton, of neutron and of valence nucleon with parameter set NL3 are plotted in figs. 1, 2 and 3.

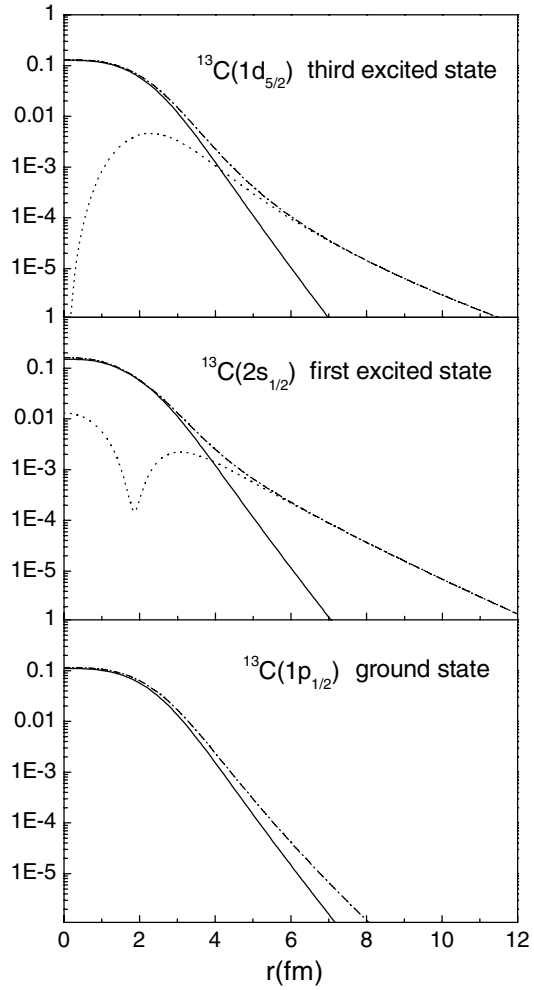

Fig. 3. The density distributions of proton, neutron, and the last nucleon for the ground state, the first and the third excited states of ^{13}C with NL3. Solid, dash-dotted, and dotted curves represent the density distributions of proton, neutron, and the last neutron for ^{13}C, respectively.

4 Discussion

Up to now, there has not been a uniquely quantitative definition on neutron (proton) halo and skin, though the two concepts are widely used. A well-accepted definition on halo and on skin is still pending. Furthermore there is no quantitative criterion to distinguish between halo and skin. In order to make a clear conclusion of the existence of halo or skin, people have to combine all the possible experimental data and theoretical results, such as the density distributions, the nuclear radii, the binding energy, separation energy, the spin and parity etc. Even if the problem to define the halo and skin has not been completely solved, some conditions are required to prove the appearance of halo or skin in a nucleus. It is agreed that the skin is a general phenomenon for many nuclei near (or off) the stable line. The skin may involve the participation of the nucleons whose number varies from a few to many. However, the halo is a specific phenomenon for the ground states in exotic nuclei near the drip line and its appearance

originates from the contribution of few weakly bound nucleons. In this paper, our criterion for the appearance of halo in the excited state of a nucleus is as follows: 1) the excited states are mainly the S states; 2) there is a long tail for the valence nucleon density distribution of a nucleus; 3) the root-mean-square (RMS) radius of the last nucleon is evidently larger than that of the other nucleons. Usually we call a nucleus as a skin nucleus if condition 1) is not fulfilled and conditions 2) and 3) are partly fulfilled. Our criterion is equivalent to that of Fukunishi [47], Otsuka [48], and Tanihata [14,39] to some extent. At present it is believed that the above criterion and differentiation are better than a simple expression. Of course, it is necessary to give a quantitative expression to show halo and skin phenomena by combining all factors in the future.

We first consider the results for the heavier mirror nuclei ^{15}N-^{15}O and ^{21}Na-^{21}Ne, deferring discussion for those of ^{13}N-^{13}C to later on (since the two lowest excited states of ^{13}N are both unbound).

4.1 ^{15}N-^{15}O

It can be seen that from tables 1 and 2, the RMF calculations with two different parameter sets can reproduce well the binding energies of ^{15}N-^{15}O as a whole. The differences between theoretical binding energies and experimental ones for the ground states are less than 1.00 MeV and the corresponding relative error is about 0.5%. Of course, a better precision is expected for the description of a successful parameter set. It is well known that the two parameter sets NL3 and NLZ are determined by fitting the experimental properties of several standard spherical nuclei, such as ^{16}O and ^{40}Ca etc. It is inevitable that, to some extent, a discrepancy between experiment and calculation occurs when the two parameter sets are applied to the approach for an open-shell nucleus. In the case of the excited states, the agreement is not so good and the largest relative difference is 2.5% off (see the result with NLZ for the $1d_{5/2}$ excited state in ^{15}O). But one should note that all these results are obtained without readjustment of any parameter. The experimental data for energy levels show that $1d_{5/2}$ and $2s_{1/2}$ are the first and the second excited states for ^{15}N, respectively, whereas the order is reverse in ^{15}O [45]. For both parameter sets, the calculated results for the $1d_{5/2}$ excited state ^{15}N, are almost same as those for its ground state ($1p_{1/2}$), except for the smaller single-particle energy of the valence proton. It shows that there is not any exotic structure in the $1d_{5/2}$ excited state of ^{15}N. But the situation is significantly different when one looks at the results in tables 1 and 2, for the $2s_{1/2}$ excited state of ^{15}N, where the RMS radius of the last proton is 4.79 fm for NL3 and 4.66 fm for NLZ. They are much larger than the respective matter radius, 2.75 fm and 2.82 fm. In addition, both $|R_p - R_n|$ (0.29 fm for NL3 and 0.24 fm for NLZ) and R_{LP}/R_m (1.74 for NL3 and 1.65 for NLZ) for the $2s_{1/2}$ excited state are much larger than those for the ground state where they are both 0.06 fm and 1.13 for NL3 and NLZ, respectively. The single-particle energies for ^{15}N listed in tables 1 and 2 show that the last proton is tightly bound in the ground state (-11.22 MeV for NL3 and -11.28 for NLZ) and weakly bound in the $2s_{1/2}$ excited state (-0.88 MeV for NL3 and -1.67 MeV for NLZ). Furthermore, we plot in fig. 1, the density distributions of proton, neutron and the last proton in ^{15}N. It is obvious that the proton density distribution for the $2s_{1/2}$ excited state has a long tail compared with that for the $1d_{5/2}$ excited state. Therefore, this suggests that there exists a proton halo in the $2s_{1/2}$ excited state of ^{15}N.

The results obtained with NL3 for ^{15}O are also listed in table 1 for comparison with ^{15}N. For the $2s_{1/2}$ excited state, the valence neutron RMS radius is 4.30 fm, which is much larger than the matter RMS radius, 2.67 fm and this leads to a large ratio, $R_{LP}/R_m = 1.61$. It is smaller than but still close to the corresponding value in the $2s_{1/2}$ excited state of ^{15}N, 1.70. However, the difference of RMS radius between proton and neutron is only 0.14 fm, which is a bit larger than that of the ground state, 0.11 fm, but is rarely smaller than that for the $2s_{1/2}$ excited state of its mirror nucleus ^{15}N, 0.25 fm. Moreover, the single-particle energy of the last neutron is -3.58 MeV, and its absolute value is relatively larger than that for the $2s_{1/2}$ excited state of ^{15}N, -0.88 MeV. Hence it is suggested that there might be a neutron skin in the $2s_{1/2}$ excited state of ^{15}O. In addition, it can be seen from fig. 1 that the neutron density distribution in the $2s_{1/2}$ excited state of ^{15}O is obviously diffuse compared with that in the ground state, however the difference between neutron and proton density distributions is not very large and this confirms the formation of the neutron skin. The case in the $1d_{5/2}$ excited state of ^{15}O is the same as that for the $1d_{5/2}$ excited state of ^{15}N, in which there is no exotic structure. For the calculations for ^{15}N-^{15}O with NLZ force, the same conclusion can be drawn so we do not repeat it here.

4.2 ^{21}Na-^{21}Ne

The results obtained with NL3 for ^{21}Na-^{21}Ne are shown in table 3 and fig. 2. The agreement between the calculated binding energies and the experimental ones is not as good as that for ^{15}N-^{15}O. The binding energies are underestimated by several MeV by the RMF model in all case. As mentioned above, this could mainly arise from the large deformations for $A \sim 20$ nuclei. Although the spherical code can give an approximate description of these largely deformed nuclei, it is necessary to perform further study on them with the deformed model in the future. One can see that the difference of RMS radius between proton and neutron in the $2s_{1/2}$ excited state of ^{21}Na is 0.25 fm. The corresponding valence proton radius and the ratio of the RMS radius of proton to neutron reach 4.50 fm and 1.57, respectively. The former quantity can fulfill the above criterion for the formation of halo, while the latter is a little small. The single-particle energy of the valence proton is -1.09 MeV, which indicates that the $2s_{1/2}$ excited state of ^{21}Na is weakly bound. So this suggests that there is a proton skin (or a pigmy proton halo) in the $2s_{1/2}$ excited state of ^{21}Na. The conclusion can also be proved by the

density distributions plotted in fig. 3. For its mirror nucleus ^{21}Ne, one can see that in the same table and figure, the situation is different and there is no exotic structure in the $2s_{1/2}$ excited state.

4.3 ^{13}N-^{13}C

We first consider the structure of ^{13}C and then we will give a discussion for ^{13}N, in which the $2s_{1/2}$ and the $1d_{5/2}$ excited states are both unbound resonances. Since the properties for the $2s_{1/2}$ excited state in ^{13}C has been calculated previously [31], here we just put emphasis on the $1d_{5/2}$ excited state of ^{13}C. The RMS radius of the valence neutron in the $1d_{5/2}$ excited state of ^{13}C is 3.88 fm. It agrees with the corresponding experimental result (3.68 ± 0.40 fm) within the error bar, ref. [29], where it was declared that there is a neutron skin in the $1d_{5/2}$ excited state of ^{13}C. The single-particle energy (-0.33 MeV) of the valence neutron is small and it indicates that the $1d_{5/2}$ excited state of ^{13}C is weakly bound compared with the ground state [44,45]. At the same time, it should be noted that although the calculated $|R_p - R_n|$ (0.29 fm) and R_{LP}/R_m (1.61) are both large, the above RMS radius of the valence neutron is too small. Moreover considering the large centrifugal barrier of the $1d_{5/2}$ shell, it suggests that, as done by Liu *et al.*, a neutron skin can form in the $1d_{5/2}$ excited state of ^{13}C.

Before we give a discussion of ^{13}N, let us make the comparison of halo or skin size between mirror nuclei. The ratios of the last nucleon RMS radius to the matter one are plotted in fig. 4. For comparison, some known ratios of other exotic nuclei are also given in the same figure. It should be noted that the results for all the nuclei in fig. 4 are from RMF calculations except for that of ^{11}Li, which is from experimental data [1,49]. It is clearly seen that the value 1.5 may be looked at as a dividing line. For those cases that have (or not) exotic structure, the ratios are all larger (or smaller) than 1.5. For ^{12}B [31], the larger ratio reaches 2.08, which is even larger than that of the well-tested exotic nucleus ^{11}Li, 1.87. For the other couple of mirror nuclei ^{17}F-^{17}O, in which exotic structures exist in the $2s_{1/2}$ excited states [28,31], the same rule can be seen obviously. Based on the above observation, we suggest that the ratio size can be regarded as an additional criterion for the formation of halo or skin. It is interesting that the ratios for the excited states of ^{15}N, ^{17}F and ^{21}Na are all consistently larger than those of their respective mirror partners ^{15}O, ^{17}O and ^{21}Ne. In addition, the ratio for the excited state decreases monotonously with mass number due to the decrease of proportion of the last nucleon in a nucleus, whereas that for the ground state has no such behavior, and vibrates around a value of about 1.25.

Finally, let us discuss briefly the case of ^{13}N. From the single-particle energy of the valence proton for ^{13}N listed in table 4, we know that the $2s_{1/2}$ and the $1d_{5/2}$ excited states of ^{13}N are both unbound which is consistent with the experimental results [44,45]. This shows that the RMF code can predict properly the unbound excited states of ^{13}N. As well known, a wave function for an unbound resonance is not square integrable and must therefore lead to an infinitely large RMS radius. So here only the binding energies are given and all kinds of radii and corresponding density distributions are omitted. Up to now, there has been no detailed study on the exotic structure in an unbound state. However, in view of the fact that the size of proton halo or skin is larger than that of neutron halo or skin in each couple of mirror nuclei, one expects that this rule will hold for ^{13}N-^{13}C, namely, there is an unbound proton halo and skin in the $2s_{1/2}$ and the $1d_{5/2}$ excited states of ^{13}N, respectively.

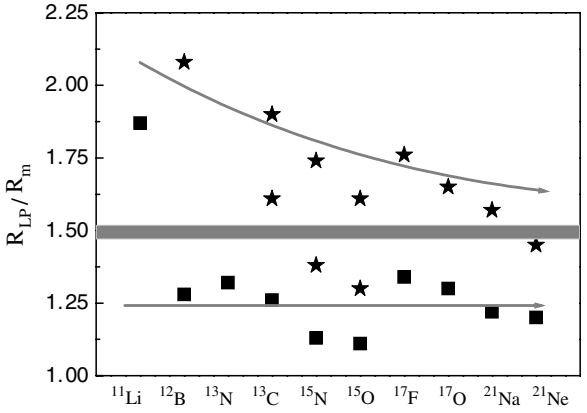

Fig. 4. The ratios of the last nucleon RMS radius to the matter one for the ground states and the excited states in some exotic nuclei. The squares indicate the ratios in the grounds while the stars are for those in the excited states. The result for ^{11}Li is taken from refs. [1,49] and those for ^{12}B and for the ground and first excited states of ^{13}C, and for ^{17}F-^{17}O are taken from ref. [31] and ref. [28], respectively.

5 Conclusion

To summarize, we have calculated the properties of three pairs of mirror nuclei with a good inert core plus one unpaired nucleon outside the core by using the framework of nonlinear relativistic mean field with NL3 and NLZ force parameters. Both parameter sets can yield almost similar results and can reproduce the experimental binding energies well except for largely deformed nuclei. The calculations show that the $2s_{1/2}$ and the $1d_{5/2}$ excited states of ^{13}N are both unbound while the $1d_{5/2}$ excited state of ^{13}C, the $2s_{1/2}$ excited states of ^{15}N, of ^{15}O and of ^{21}Na are all weakly bound. It is predicted that there is a neutron skin in the $2s_{1/2}$ excited states of ^{13}C and of ^{15}O, respectively. It is also shown that there exists a proton halo and a proton skin (or a pigmy proton halo) in the $2s_{1/2}$ excited states of ^{15}N and of ^{21}Na, respectively. For ^{13}N, there could be a proton halo and a proton skin in the $2s_{1/2}$ and the $1d_{5/2}$ unbound excited resonances, respectively. It is necessary to perform relevant experiments for the confirmation of our theoretical prediction.

This work was supported by the Major State Basic Research Development Program under Contract No. G2000077404, by the National Natural Science Foundation of China under Contract No. 10125521, by the fund of Education Ministry of China under Contract No. 20010284036 and by Shanghai Phosphor Program Under Contract Number 03 QA 14066.

References

1. I. Tanihata, H. Hamagaki, O. Hashimoto, Y. Shida *et al.*, Phys. Rev. Lett. **55**, 2676 (1985).
2. P.G. Reinhard, M. Rufa, J. Maruhn, W. Greiner *et al.*, Z. Phys. A **323**, 13 (1986).
3. B.D. Serot, J.D. Walecha, Adv. Nucl. Phys. **16**, 1 (1986).
4. W. Mittig, J.M. Chouvel, W.L. Zhan, L. Bianchi *et al.*, Phys. Rev. Lett. **59**, 1889 (1987).
5. P.G. Reinhard, Rep. Prog. Phys. **52**, 439 (1989).
6. M.G. Saint-Laurent *et al.*, Z. Phys. A **332**, 457 (1989).
7. M. Rufa, P.G. Reinhard, J.A. Maruhn, W. Greiner, M.R. Strayer, Phys. Rev. C **38**, 390 (1989).
8. E. Liatard *et al.*, Europhys. Lett. **13**, 495 (1990).
9. Y.K. Gambhir, P. Ring, A. Thimet, Ann. Phys. (N.Y.) **198**, 132 (1990).
10. B.A. Brown, Phys. Rev. C **43**, R1513 (1991).
11. L.S. Warrier, Y.K. Gambhir, Phys. Rev. C **49**, 871 (1991).
12. W. Koepf, Y.K. Gambhir, P. Ring, M.M. Sharma, Z. Phys. A **340**, 119 (1991).
13. A.C.C. Villari, W. Mittig, E. Plagnol, Y. Schutz *et al.*, Phys. Lett. B **268**, 345 (1991).
14. I. Tanihata, D. Hirata, T. Kobayashi, S. Shimoura *et al.*, Phys. Lett. B **289**, 261 (1992).
15. D. Hirata, H. Toki, I. Tanihata, P. Ring, Phys. Lett. B **314**, 168 (1993).
16. M.V. Zhukov, B.V. Danilin, D.V. Fedorov, J.M. Bang *et al.*, Phys. Rep. **231**, 151 (1993).
17. Y. Sugahara, H. Toki, Nucl. Phys. A **579**, 557 (1993).
18. K. Varga, Y. Suzuki, Y. Ohbayasi, Phys. Rev. C **50**, 189 (1994).
19. Y.K. Gambhir, Nucl. Phys. A **570**, 101 (1994).
20. R.E. Warner, J.H. Kelley, P. Zecher, F.D. Becchetti *et al.*, Phys. Rev. C **52**, R1166 (1995).
21. F. Negoita, C. Borcea, F. Carstoiu, M. Lewitowicz *et al.*, Phys. Rev. C **54**, 1787 (1996).
22. B. Blanka, C. Marchanda, M.S. Pravikoffa, T. Baumannb *et al.*, Nucl. Phys. A **624**, 242 (1997).
23. G.A. Lalazissis, A.R. Farhan, M.M. Sharma, Nucl. Phys. A **628**, 221 (1998).
24. Z.Z. Ren, W. Mittig, F. Sarazin, Nucl. Phys. A **652**, 250 (1999).
25. E. Sauvan, F. Carstoiu, N.A. Orr *et al.*, Phys. Lett. B **491**, 1 (2000).
26. I.J. Thompson, Nucl. Phys. A **701**, 7 (2002).
27. R. Morlock, R. Kunz, A. Mayer, M. Jaeger *et al.*, Phys. Rev. Lett. **79**, 3837 (1997).
28. Z.Z. Ren, A. Faessler, A. Bobyk, Phys. Rev. C **57**, 2752 (1998).
29. Z.H. Liu, C.J. Lin, H.Q. Zhang, Z.C. Li *et al.*, Phys. Rev. C **64**, 034312 (2001).
30. C.J. Lin, Z.H. Liu, H.Q. Zhang, Y.W. Wu *et al.*, Chin. Phys. Lett. **18**, 1183 (2001).
31. Z.Z. Ren, W.Z. Jiang, X.Z. Cai, Z.Y. Zhu *et al.*, Commun. Theor. Phys. **38**, 470 (2002).
32. K. Arai, Y. Suzuki, K. Varga, Phys. Rev. C **51**, 2488 (1995).
33. Z.H. Li, W.P. Liu, X.X. Bai, Y.B. Wang *et al.*, Phys. Lett. B **527**, 50 (2002).
34. S. Marcos, N. Van Giai, L.N. Savushkin, Nucl. Phys. A **549**, 143 (1992).
35. J. Horowitz, B.D. Serot, Nucl. Phys. A **368**, 503 (1981).
36. S.K. Patra, Nucl. Phys. A **559**, 173 (1993).
37. Z.Z. Ren, M. Mittig, B.Q. Chen, Z.Y. Ma, Phys. Rev. C **52**, 20 (1995).
38. R.J. Furnstahl, C.E. Price, Phys. Rev. C **40**, 1398 (1989).
39. I. Tanihata, D. Hirata, H. Toki, Nucl. Phys. A **583**, 769 (1995).
40. M.M. Sharma, M.A. Nagarajan, P. Ring, Phys. Lett. B **312**, 377 (1993).
41. G.A. Lalazissis, J. König, P. Ring, Phys. Rev. C **55**, 540 (1997).
42. R. Sherr, G. Bertsch, Phys. Rev. C **32**, 1809 (1985).
43. I. Tanihata, T. Kobayashi, O. Yamakawa, S. Shimoura *et al.*, Phys. Lett. B **206**, 592 (1988).
44. G. Audi, A.H. Wapstra, At. Mass Eval. **32**, 1809 (1993).
45. F. Ajzenberg-Selove, Nucl. Phys. A **523**, 1 (1991).
46. P.M. Endt, Nucl. Phys. A **633**, 1 (1998).
47. N. Fukunishi, T. Otsuka, I. Tanihata, Phys. Rev. C **48**, 1648 (1993).
48. T. Otsuka, N. Fukunishi, H. Sagawa, Phys. Rev. Lett. **70**, 1385 (1993).
49. L. Johannsen, A.S. Jensen, P.G. Hansen, Phys. Lett. B **244**, 357 (1990).